

# Time-of-Flight Flow Microsensor using Free-Standing Microfilaments

Roberto Jacobe Rodrigues<sup>1,2</sup>, and Rogério Furlan<sup>3</sup>

<sup>1</sup> Center of Engineering and Social Sciences, Federal University of ABC, SP, Brazil

<sup>2</sup> Laboratory of Integrated Systems, University of Sao Paulo, SP, Brazil

<sup>3</sup> Department of Physics and Electronics, University of Puerto Rico, Humacao, PR  
e-mail: roberto.rodrigues@ufabc.edu.br

## ABSTRACT

In this work we present the processing conditions and the characterization results of a time-of-flight (TOF) flow microsensor implemented using polysilicon microfilaments. Numerical simulation (ANSYS®/FLOTRAN®) and experimental results for analysis with air flow and nitrogen are compared considering different heater to sensor distances and flows. A good agreement was observed between experimental and simulated results. However, experimental TOF values resulted ever consistently higher than the simulated ones due to delays introduced by the circuitry and the data acquisition system and also in the thermal response of the microfilament. Analysis of the heater microfilament reveal that temperatures of the order of 100 °C (that is low enough to not affect the gas flow) can be obtained with a power dissipation of tens of mW. The time-of-flight measurements show that the proposed structure is suitable for the detection of low volumetric flows (tens of SCCM) and presents a response time of the order of milliseconds.

**Index Terms:** time-of-flight, flow, microsensor, surface micromachining, microsystem.

## 1. INTRODUCTION

The use of Micro-Electro-Mechanical-Systems (MEMS) technology has made possible the development of different types of flow microsensors. These devices find application in many important areas as process and environmental control, biomedicine and instrumentation [1] [2] [3].

In thermal flow microsensors that operate according to the calorimetric principle [4] [5] [6], the mass or volume flow modifies the temperature profile around a heater element. This change in temperature profile is then converted into an electrical signal by two sensors positioned upstream and downstream to the heater [4] [6] [7]. Another important principle is the thermal time-of-flight (TOF) [7] [8]. In this case a transient temperature profile is generated by an electrical pulse applied to the heater element and is detected by a downstream sensor, as presented in Figure 1. The time between the heat pulse generation and its detection (time-of-flight) can be used for flow measurement [8][9].

In reference [9] we proposed the design of a new thermal flow microsensor that combines the possibility of flow measurement using the calorimetric

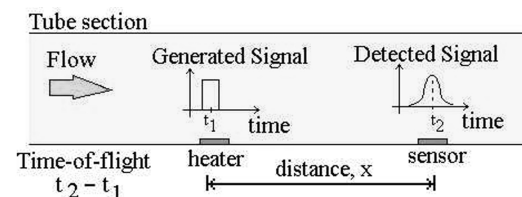


**Figure 1.** Flow measurement by TOF principle [9].

and time-of-flight principles and presented preliminary results that validate its dynamical numerical simulation. In this work we present its complete fabrication sequence, the characterization of the heater microfilament and the comparison of numerical simulation and experimental results considering different heater to sensor distances and flows and operation as a time-of-flight flow sensor.

## 2. NUMERICAL SIMULATION

Two dimensional numerical simulations were conducted using the commercial software ANSYS®/FLOTRAN® with FLOTRAN141® [10] as element type. Simulation was validated in reference [9] con-

sidering the analytical model presented by Lammerink et al [7]. The values of the thermal parameters and physical properties for thin films layers were those suggested by CRC Handbook [11] and Incropera [12]. As the adopted velocities and the air flow do not cause the decreasing of the heater temperature [6][13] the power dissipation consideration was not included in the FEM simulations. The conduction predominance for lower velocities and the convection predominance for higher velocities were considered in the simulations performed [8][9][10]. The radiation effects was not included in the model due to reduced power dissipation [6][7].

The simulated structure is presented in Figure 2. The heater filament is composed of a layer of polysilicon on top of silicon nitride. Figure 3 defines the timing adopted in the simulations. Air flow was analyzed considering ambient temperature,  $T_0 = 273$  K, heater temperature,  $T_{ht} = 473$  K, and heating pulse width,  $t_0 = 200$  ms.

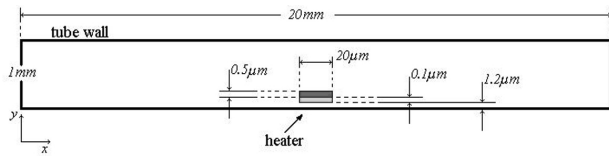


Figure 2. Tube and geometry defined for dynamic numerical simulation.

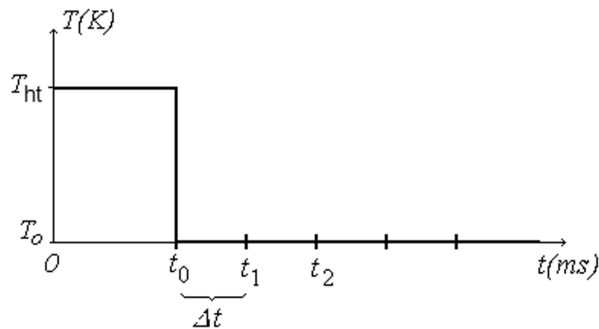


Figure 3. Thermal pulse applied on the heater element.

Curves of temperature as a function of position (heater to filament distances from 210  $\mu\text{m}$  to 1038  $\mu\text{m}$ ) having time as a parameter (intervals of 0.1 ms) were obtained, considering a fixed volumetric flow, as presented in Figure 4.

From these curves we obtained the curves of temperature as a function of time having distance from heater filament as a parameter. For each of these curves the TOF (necessary time to achieve the maximum temperature at a certain position) was obtained. This process was repeated for different volumetric flows allowing obtaining the curves presented in Figure 5.

As can be seen, this structure is suitable for the detection of low volumetric flows and presents a response time of the order of milliseconds.

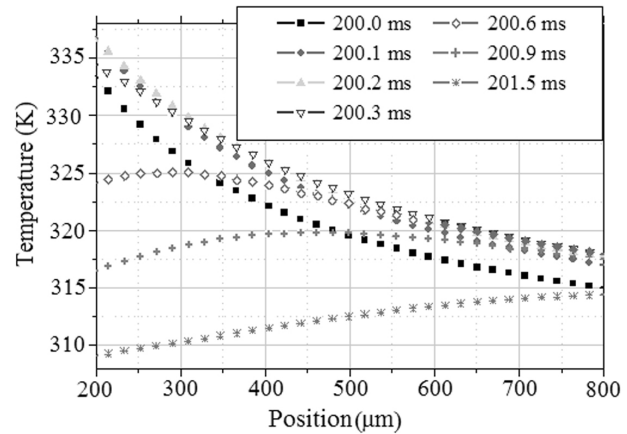


Figure 4. Curves of temperature as a function of position.

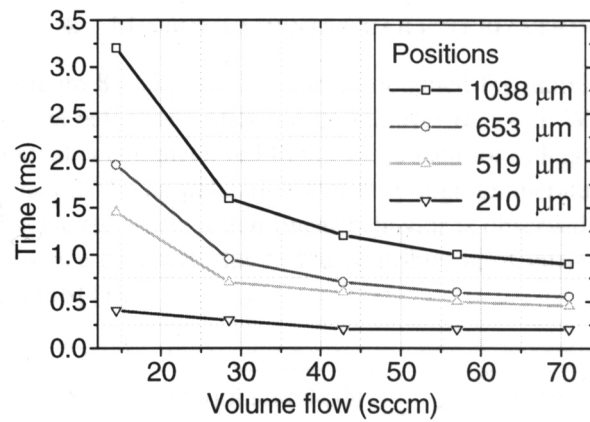


Figure 5. Time-of-Flight as a function of volumetric air flow considering different distances from the heater to the sensor.

### 3. DEVICE FABRICATION

Figure 6 presents the schematic cross-section of a device, for illustration of the fabrication sequence.

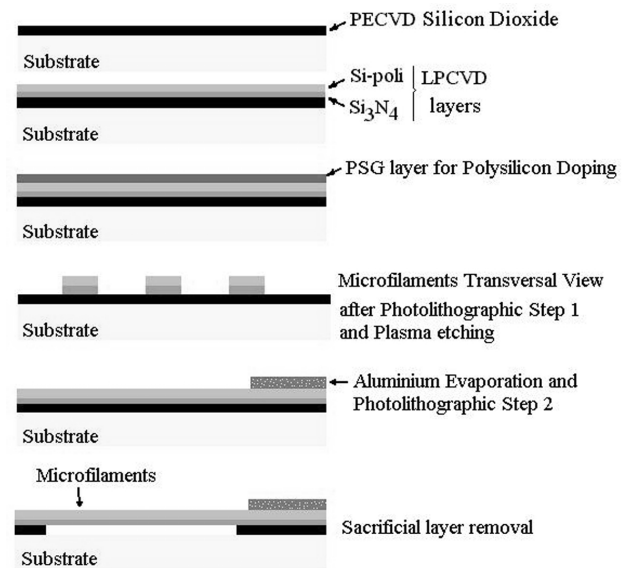


Figure 6. Main process steps for fabrication of the flow microsensor for transversal and longitudinal views of the filaments.

## Time-of-Flight Flow Microsensor using Free-Standing Microfilaments

Rodrigues & Furlan

Silicon wafers were used as substrates. Firstly, a layer of about 1.2  $\mu\text{m}$  of PECVD oxide was deposited in TEOS (Tetra-Ethyl-Ortho-Silicate) ambient, which serves as a sacrificial layer [14] [15]. The deposition conditions are presented in the Table I.

**Table I.** Conditions of deposition by PECVD of the sacrificial layer.

Adjusted condition	Adjusted values
Chamber temperature ( $^{\circ}\text{C}$ )	400
Pressure (Torr)	5
$\text{O}_2$ , TEOS and Ar flow (sccm)	40, 15 and 100
RF Power (watts)	400
Process time (minutes)	2.5

In the sequence, layers of  $\text{Si}_3\text{N}_4$  and polysilicon were deposited by LPCVD, with thicknesses of about 0.1  $\mu\text{m}$  and 0.5  $\mu\text{m}$ , respectively. The LPCVD conditions are presented in the Table II. The polysilicon doping was performed using phosphorus silicate glass (PSG) diffusion (1150  $^{\circ}\text{C}$ , 10 minutes) resulting a sheet resistance of around 68  $\Omega/\text{square}$ .

**Table II.** LPCVD conditions.

Adjusted condition	Adjusted values	
	Silicon nitride layer	Polysilicon layer
Temperature ( $^{\circ}\text{C}$ )	720	630
Pressure (mTorr)	500	500
Gases concentrations	16 $\text{NH}_3$ : 1 $\text{SiH}_2\text{Cl}_2$	4 $\text{N}_2$ : 1 $\text{SiH}_4$

**Table III.** Plasma etching conditions.

Adjusted condition	Adjusted values
Chamber Pressure (mTorr)	50
$\text{SF}_6$ , Ar and $\text{H}_2$ flow (sccm)	10, 20 and 15
RF Power (watts)	100
Process time (minutes)	20

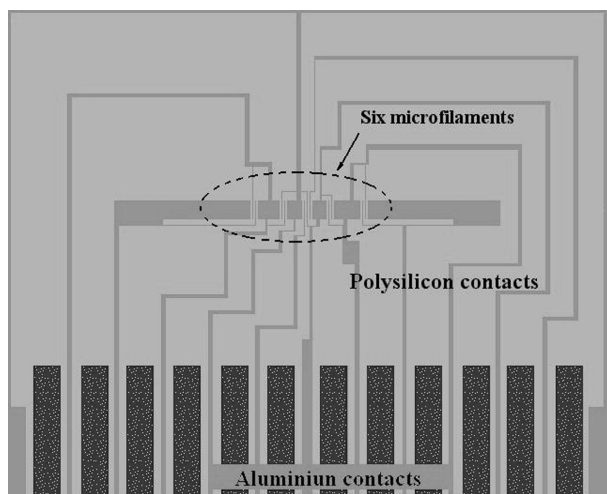


**Figure 7.** Schematic representation of the top view of the microsensor.

The first photolithographic step (conventional microelectronics process) and plasma etching (conditions presented in Table III) were performed for polysilicon electrical contacts and microfilaments definition. The aluminum layer was deposited by evaporation (thickness around 0.5  $\mu\text{m}$ ) and patterned to form electrical contacts through conventional wet chemical etching after the second photolithographic step.

The wafers were cut for devices definition. Then the sacrificial layer removal was performed in DLV solution ( $6\text{NH}_4\text{F} + 1\text{HF}$ ) in a time of approximately 50 minutes. Figure 7 shows a schematic representation of the top view of the device, which results after the fabrication process.

## 4. MICROFILAMENTS CHARACTERIZATION

Figure 8 compares I-V curves obtained for individual filaments before and after sacrificial layer removal. When the removal is complete, red light can be seen for voltages higher than 27 V, an indication that very high temperatures can be achieved. Also, a non-linear behavior is observed, with a resistance decrease, due to the contribution of intrinsic carriers [16] [15].

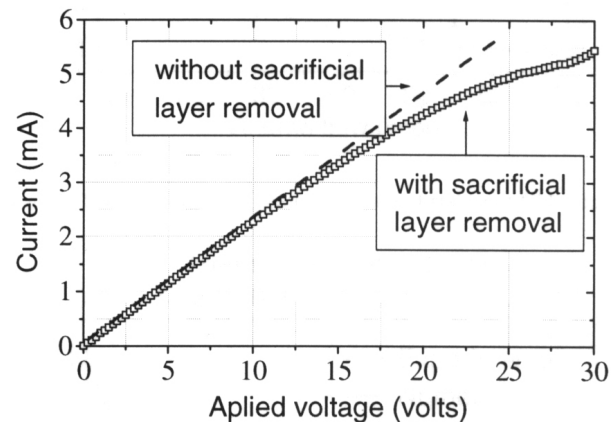


**Figure 8.** I-V curves before and after sacrificial layer removal.

In order to obtain a temperature of the order of 100  $^{\circ}\text{C}$ , that is low enough to not affect the gas flow, a voltage of the order of 12 V has to be applied to the heater, resulting a power dissipation of the order of 30 mW.

## 5. FLOW SENSOR CHARACTERIZATION

After fabrication, the sensor was mounted on the bottom of a flow channel with a circular cross-section with 1 mm of the diameter and a length of 20 cm. This structure was connected in series with a commercial mass flow meter, as shown in Figure 9.

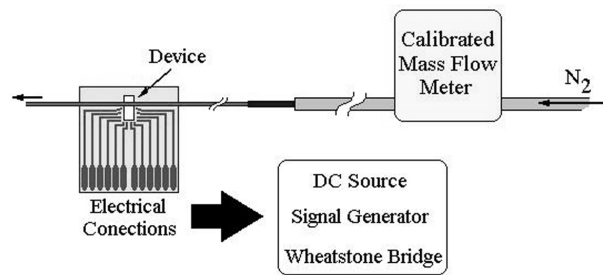


Figure 9. Experimental Setup.

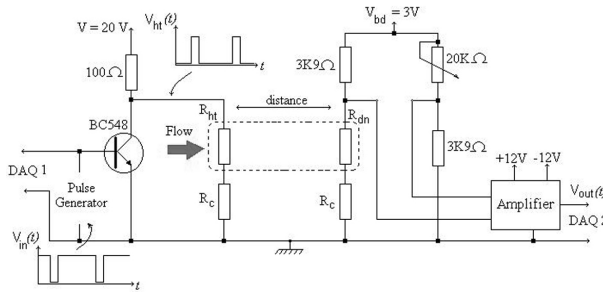


Figure 10. Schematics of the electronics circuit used for application of pulses in the heater filament and for detection.

Figure 10 shows the electronic circuit used. The pulses coming from the signal generator are applied to the contacts of the heater filament. For detection of variations of the resistance of the sensor microfilament ( $R_{dn}$ ) a Wheatstone bridge was used. The output of the bridge was amplified a thousand times using an instrumentation amplifier.

A data acquisition system was used to store the output of both the input generator and of the output amplifier as a function of the time. The TOF was defined as the delay between these two signals. The signal obtained from the data acquisition system ( $V_{out}$ , Figure 10) was treated and analyzed in a way to permit the comparison with the pulses applied to the heater ( $V_{ht}$ ). Figure 11 illustrates the method used to experimentally determine the delay until the change in behavior of  $V_{out}$  after the transition of the input pulse  $V_{ht}$ . This measured delay corresponds to the TOF and it was measured for each adjusted volume flow value. Figures 12 and 13 present the TOF as a function of flow rate, for heater to sensor distances of 544  $\mu\text{m}$  and 1038  $\mu\text{m}$ , respectively. A good agreement is observed with respect to the numerical simulation, confirming the predicted behavior. The experimental TOF values are ever consistently higher than the simulated ones due to delays introduced by the circuitry and the data acquisition system and also in the thermal response of the microfilament. Noise and variations of the temperature of the filament can be considered as the main causes for the fairly large size of the error bars in Figures 12 and 13. The coupling of the microsensor with an integrated amplifier could help to reduce the noise.

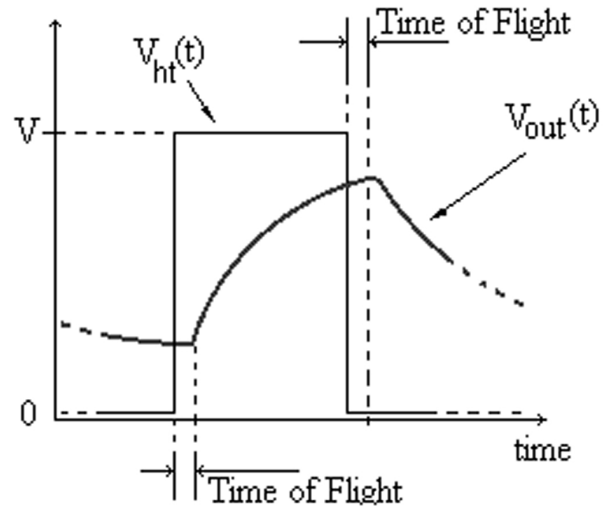


Figure 11. Illustration showing the pulse applied at the heater ( $V_{ht}$ ) and the signal due to the variation of temperature around the sensor microfilament ( $V_{out}$ ) that is obtained using the circuit presented in Figure 10.

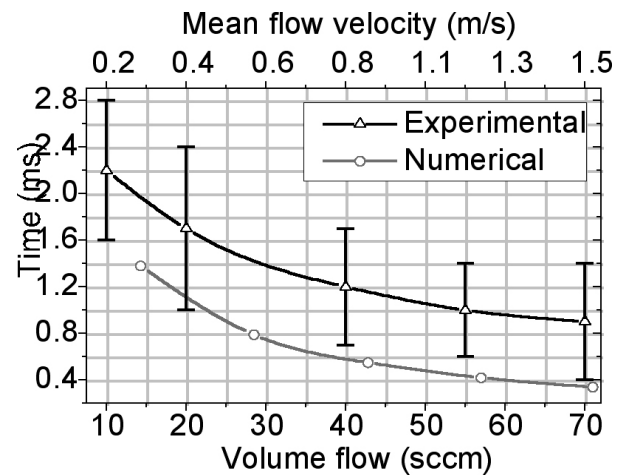


Figure 12. Time-of-Flight for heater-to-sensor distance of 544  $\mu\text{m}$ .

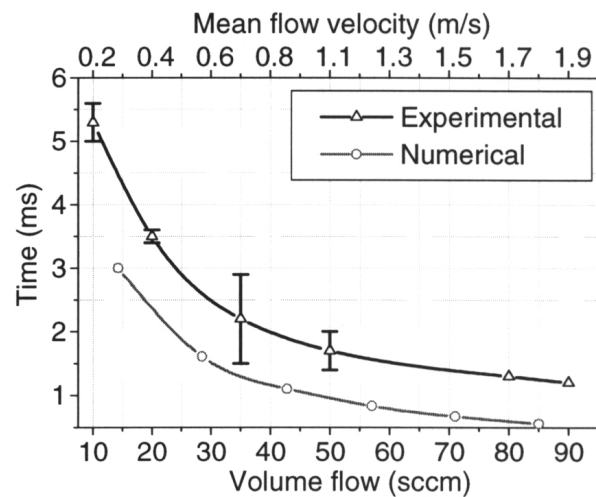


Figure 13. Time-of-Flight for heater-to-sensor distance of 1038  $\mu\text{m}$ .

## 6. CONCLUSIONS

In this work we presented the numerical analysis, the implementation and the characterization of a flow sensor structure fabricated using surface micro-machining in combination with sacrificial layer technology. This approach allows obtaining free-standing polysilicon microfilaments that can be used as heaters or temperature sensors. Although the presented structure can be operated using both the calorimetric and the TOF principles, in this work we explored in detail the second one. Numerical simulation using the commercial software ANSYS®/FLOTRAN® showed a compromise between the size of the device (distance between heater and sensor, in the range between 210  $\mu\text{m}$  and 1038  $\mu\text{m}$ ) and the range of volumetric flow to be detected. Also, the proposed structure is suitable for the detection of low volumetric flows (lower than 100 sccm) and presents a response time of the order of milliseconds. Experimental results demonstrate that microfilaments were released from the substrate and the heater can be operated at a temperature of the order of 100 °C (that is low enough to not affect the gas flow) by using a voltage of the order of 12 V. The heater operates with a power dissipation of the order of 30 mW. Also, tests with the implemented flow sensor structure and characterization apparatus revealed a good agreement with respect to the numerical simulation, confirming the predicted behavior.

## ACKNOWLEDGEMENTS

This work was supported by FAPESP (Brazil) and PADCT/CNPq (Brazil).

## REFERENCES

- [1] A. Rasmussen et al., "Simulation and optimization of a microfluidic flow sensor," *Sensors and Actuators A*, vol. 88, Issue 2, February, 2001, pages 121 - 132.
- [2] G. Kaltsas and A. G. Nassiopoulou, "Gas flow meter for application in medical equipment for respiratory control: study of the housing," *Sensors and Actuators A*, vol. 110, Issues 1-3, February, 2004, pages 413 - 422.
- [3] A. Kohl et al., "Development of miniaturized semiconductor flow sensors," *Measurement*, vol. 33, Issue 2, March, 2003, pages 109 - 119.
- [4] E. Yoon and K. D. Wise, "An integrated mass flow sensor with on-chip CMOS interface circuitry," *IEEE Transactions on Electron Devices*, vol. 39, Issue 6, 1992, pages 1376 - 1386.
- [5] D. Moser, R. Lenggenhager, H. Baltes, "Silicon gas flow sensors using industrial CMOS and bipolar IC technology," *Sensors and Actuators A*, vol. 27, Issues 1-3, May, 1991, pages 577 - 581.
- [6] L. Qio, S. Hein, E. Obermeier and A. Schubert, "Micro-gas-flow sensor with integrated heat sink and flow guide," *Sensors and Actuators A*, vol. 54, Issues 1-3, June, 1996, pages 547 - 551.
- [7] T. S. J. Lammerink, N. Tas, R. M. Elwenspoek and J. H. J. Fluitman, "Micro liquid flow sensor," *Sensors and Actuators A*, vol. 37-38, June-August, 1993, pages 45 - 50.
- [8] M. Ashauer et al., "Thermal flow sensor for liquids and gases based on combinations of two principles," *Sensors and Actuators A*, vol. 73, Issues 1-2, March, 1999, pages 7 - 13.
- [9] R. J. Rodrigues and R. FURLAN, "Design of microsensor for gases and liquids flow measurements," *Microelectronics Journal*, vol. 34, Issues 5-8, May-August, 2003, pages 709 - 711.
- [10] *Technical OverView*, Ansys Corporation, 1996.
- [11] CRC HandBook of Chemistry and Physics: A Ready - Reference Book of Chemical and Physical Data, CRC Press, 78.ed., New York: 1998.
- [12] Incropera, F.P. and DeWitt, D.P., *Fundamentals of Heat and Mass Transfer*, John Wiley and Sons, 4.ed., 1996.
- [13] Nguyen, N. T. and Kiehnscherf, R. "Low-cost silicon sensors for mass flow measurement of liquids and gases," *Sensors and Actuators A*, vol. 49, Issues 1-2, June, 1995, pages 17 - 20.
- [14] M. J. Madou, *Fundamentals of microfabrication: The science of miniaturization*, 2.ed., CRC Press, 2002.
- [15] E. W. Simões et al., "Fabrication process of free-standing polysilicon microfilaments using PECVD silicon oxide as a sacrificial layer," in *Technical Digest, Micromechanics Europe*, U.K., 1997, pages 47-50.
- [16] R. J. Rodrigues and R. Furlan, "Microsensor for liquid flow measurements," in *Proceedings of the 15th International Conference on Microelectronics and Packaging*, 2000, Manaus, Brazil, pages 390 - 393.